IEEE Access
Multidisciplinary ⋮ Rapid Review ⋮ Open Access Journal

Received November 19, 2021, accepted December 10, 2021, date of publication December 15, 2021,
date of current version December 24, 2021.

Digital Object Identifier 10.1109/ACCESS.2021.3135810

Compressed Sampling in Shift-Invariant Spaces Associated With FrFT

HAORAN ZHAO[1,2,3], LEI ZHANG[1,2,3], (Member, IEEE), AND LIYAN QIAO[4], (Member, IEEE)

[1]School of Integrated Circuits, Tsinghua University, Beijing 100084, China
[2]Beijing Innovation Center for Future Chips, Tsinghua University, Beijing 100084, China
[3]Beijing National Research Center for Information Science and Technology, Tsinghua University, Beijing 100084, China
[4]Automatic Test and Control Institute, Harbin Institute of Technology, Harbin 150001, China

Corresponding author: Lei Zhang (zhang.lei@tsinghua.edu.cn)

This work was supported in part by the National High Technology Research and Development Program of China under Grant 2020YFB1805004, and in part by the National Natural Science Foundation of China under Grant 61941103.

ABSTRACT Shift-invariant and sampling spaces play a vital role in the fields of signal processing and image processing. In this paper, we extend the generalized shift-invariant and sampling subspaces from the traditional sampling spaces to the compressed sampling, and develop a compressed sampling method for analog sparse signals based on the shift-invariant spaces associated with fractional Fourier transform (FrFT). First, we show the generalized shift-invariant and sampling subspaces can be used to explain the traditional sampling spaces with single generator or multiple generators in the fractional Fourier domain (FrFD). The non-ideal sampling structures of single channel and multiple channels are special cases of the generalized shift-invariant subspaces. Second, a compressed sampling method for the sparse signals in the FrFD is proposed by reusing the multiple generators of the shift invariant spaces as sparse representation. We combine the sensing matrix of compressed sensing and the framework of sampling scheme in the shift-invariant spaces to construct a compressed sampling method, which perfectly recovered the original signal with a sufficient low sampling rate. By choosing different filters, the proposed framework allows to derive many specific sampling schemes. Finally, a compressed sampling method for multiband signals in the FrFD is proposed based on the forgoing theorems. The numeral simulation validates the theoretical derivations.

INDEX TERMS Fractional Fourier transform, fractional fourier domain, shift-invariant spaces, compressed sampling, random demodulation.

I. INTRODUCTION

Fractional Fourier transformation (FrFT) is an extension of the ordinary Fourier transform (FT). The FrFT essentially allows the signal in the time-frequency domain to be projected with an additional degree of freedom. The definition of the FrFT [1] is as follows:

$$X_\alpha(u) = \mathcal{F}^\alpha\{x(t)\}(u) = \int_{\mathbb{R}} K_\alpha(u,t)x(t)\mathrm{d}t, \tag{1}$$

where $\mathcal{F}^\alpha$ denotes the FrFT operator. The transform kernel function $K_\alpha(u,t)$ is given by:

$$K_\alpha(u,t) = \begin{cases} \varphi_\alpha \lambda_\alpha(t)\lambda_\alpha(u)e^{-jtu\csc\alpha}, & \alpha \neq k\pi, \\ \delta(u-t), & \alpha = 2k\pi, \\ \delta(u+t), & \alpha = (2k+1)\pi, \end{cases} \tag{2}$$

where $\varphi_\alpha = \sqrt{\frac{1-j\cot\alpha}{2\pi}}$. $\lambda_\alpha(\cdot) = e^{\frac{j}{2}(\cdot)^2\cot\alpha}$. $k \in \mathbb{Z}$.

The associate editor coordinating the review of this manuscript and approving it for publication was Wei Wang.

The FrFT is a powerful mathematical tool in the fields of ultra-wideband communication, radar and time-variant filtering and so on [2]–[4]. Due to the importance of the FrFT in signal and image processing, sampling theories have been developed from the traditional frequency domain (FD) to the fractional Fourier domain (FrFD) for many years. The generalized sampling model in the FrFD [5]–[7] has been proposed which used sampling and shift-invariant spaces (SISs) theory to explain most of the existing sampling models such as Xia's bandlimited sampling method [8] and other extension forms [9]–[11]. Sampling in the SISs named sampling spaces is a special class of the SISs, in which the coefficient of the generator is determined by the values of discrete points of the function. The sampling theory without bandlimited constrain is based on the discrete FrFT whose discretization is derived from the Shannon's sampling theorem with the 2π constraints. From the foregoing analysis, sampling spaces can be used to derive the new sampling kernel for the fractional Fourier

This work is licensed under a Creative Commons Attribution 4.0 License. For more information, see https://creativecommons.org/licenses/by/4.0/

bandlimited signals, that means those extensions allow to sample and reconstruct signal using a broad variety of filters [5], [12]–[14].

Union SISs theory plays an important role in signal sampling theories because the sampled signal can be expressed as linear combinations of shifts of a set of generators. The multiple generators model has been applied in many signal processing applications, such as extension of Shannon's sampling theorem [15], [16]. The multiband signals, whose energy are concentrated in the FrFD with several separated bandlimited components, can be understood as the accumulation of several bandlimited signals. Every bandlimited component of the multiband signal is represented by a generator, and all of generators are different from each other and exist in different sampling channels, then the original signal can be expressed by the summation of several generators with different coefficients, each generator could be sampled by a relatively low sampling rate.

Sampling in the SISs could be understood as using known generators or bases to represent the signal. Suppose the number and forms of the generators are known, how can we find coefficients of the generators from a known complete basis with a sufficient low sampling rate. This question is a special case of sampling a signal in a union of subspaces [17]–[19]. In our question, signals can be represented by $K < L$ generators in the SISs, but we do not know which generators are chosen, where L is the number of generators in the defined subspaces. There is no a concrete sampling methods to ensure efficient and stable recovery under this hypothesis, for example, $x(t) \in \mathcal{V}_{\alpha,\beta}(\theta_1, \cdots, \theta_L)$. Signal $x(t)$ can be represented by function set $\{\theta_1, \cdots, \theta_L\}$, but the coefficients of the generators are unknown. That means we do not know which generators are necessary. In other words, signals belong to the subspaces of $\mathcal{V}_{\alpha,\beta}(\theta_1, \cdots, \theta_L)$, then some generators are not necessary whose coefficients would be zero, in this situation, taking the generators as the bases, the signal will show sparse in $\mathcal{V}_{\alpha,\beta}(\theta_1, \cdots, \theta_L)$. In this paper, we applied compressed sensing (CS) to solve this problem in the FrFD.

Compressed sensing (CS) is also a special case of sampling on a unions of subspaces which combines the compression and the sampling at the same time [20], [21]. In CS theory, the original signal $\mathbf{x} \in \mathbb{R}^{N\times 1}$ can be projected from a high-dimensional space to a low-dimensional space $\mathbb{R}^{M\times 1}$ through a linear projection matrix $\mathbf{\Phi}$, if the original signal is sparse or have the sparsity in a transform domain. The low-dimensional space projection vector $\mathbf{y}$ contains all the information of the original signal. The original signal $\mathbf{x}$ can be recovered from measurement vector $\mathbf{y}$ accurately. It can be expressed as:

$$\begin{cases} \mathbf{y} = \mathbf{\Phi x} \\ \mathbf{x} = \mathbf{\Psi a} \end{cases} \rightarrow y = \mathbf{A}\boldsymbol{a} \text{ where } \mathbf{A} = \mathbf{\Phi\Psi}, \tag{3}$$

where $\mathbf{\Phi} \in \mathbb{R}^{M\times N}$ $(M \ll N)$ is the observation matrix (or measurement matrix) for $\mathbf{x}$. $\boldsymbol{a} \in \mathbb{C}^N$ is a linear $\mathcal{K}$-sparse representation for $\mathbf{x}$ on an appropriate sparse matrix $\mathbf{\Psi} \in \mathbb{C}^{N\times N}$. $\mathbf{A}$ is sensing matrix which combines $\mathbf{\Phi}$ and $\mathbf{\Psi}$.

In simple terms, CS is applied to determine a length N vector $\mathbf{x}$ from $M < N$ linear measurements, where $\mathbf{x}$ is known to be $\mathcal{K}$-sparse in some bases. Many efficient sampling and recovery algorithms have been studied for CS associated with the FrFT [3], but those methods are simply extended from the FD without analysis of the relationship between the sampling spaces and compressed methods. Our goal is to combine the CS and SISs to proposed a more general sampling model with a sufficiently low analog sampling rate. There are two problems to prevent us to give this theory. First, there is not a sampling model defined by multiple generators in the SISs associated with the FrFT. Second, traditional CS focuses on the recovery of the finite vectors which cannot be used to the continuous problem without discretization.

In this paper, we propose sampling and compressed sampling methods under the generalized shift-invariant spaces associated with the FrFT. In section I, some useful definitions are introduced such as the continuous form of the fractional Fourier, the classic sampling spaces with multiple generators, sampling in single generator shift-invariant spaces associated with the FrFT. The remainder of the paper is as follows. In section II, we will explain some multi-channel sampling schemes by the generalized model [7], and show the simplified multi-channel sampling theorems are special cases of the generalized model. In section III, we proposed two compressed sampling methods based the compressed sensing and framework of the generalized shift-invariant sampling spaces. One compressed method reused the sparse generator in the shift-invariant and discrete sensing matrix in the CS to solve the compressed problem of discrete problem. The other approach combining the filter and sensing matrix in the CS can be used to compressed sample signals directly. In section IV, two simulation parts are given, one is applied to validate the theorem of the generalized sampling spaces associated with the FrFT, the other is an example which is to show the proposed method is effective for multiband signals in the FrFD with a simple sampling structure.

II. GENERALIZED SAMPLING SPACES ASSOCIATED WITH THE FrFT AND NON-IDEAL SAMPLING MODELS

A. GENERALIZED SAMPLING SPACES ASSOCIATED WITH THE FrFT

Theorem 1 (Generalized SISs Associated With the FrFT): Let $\{c_\ell(\cdot)\} \in \ell^2, \{\theta_\ell(\cdot)\} \in L^2(\mathbb{R})$, $1 \le \ell \le L$ *and consider the chirp-modulated SISs of* $L^2(\mathbb{R})$.

$$\begin{aligned} &\mathcal{V}_{\alpha,\beta}(\theta_1, \cdots, \theta_L) \\ &= \left\{ x(t) = \sum_{\ell=1}^{L} \varphi_\beta \lambda_\alpha^*(t) \sum_{k=-\infty}^{+\infty} \hat{c}_{\alpha,\ell}[kT] \hat{\theta}_{\beta,\ell}(t - kT) \right\} \end{aligned} \tag{4}$$

where $\hat{\theta}_{\beta,\ell}(t - kT) = \lambda_\beta(t - kT)\theta_\ell(t - kT)$, $\hat{c}_{\alpha,\ell}(kT) = \lambda_\alpha(kT)c_\ell(kT)$

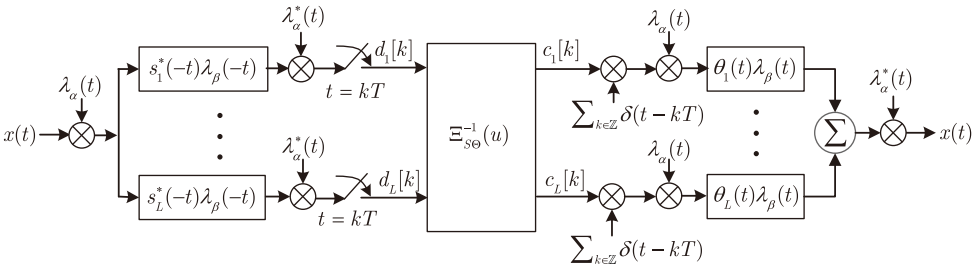

FIGURE 1. Multiple generators non-ideal sampling model in the SISs associated with the FrFT.

Then $\{\hat{\theta}_{\beta,\ell}(\cdot)\}$ *is a Riesz basis for* $\mathcal{V}_{\alpha,\beta}(\theta_1,\cdots,\theta_L)$ *if and only if there exist two positive constants* $\zeta_1,\zeta_2>0$ *such that*:

$$\zeta_1 \le \sum_{k=-\infty}^{+\infty} \left\|\Theta_{\beta,\ell}(\tilde{u}-\tilde{u}_k)\right\|^2 \le \zeta_2, \quad 1\le \ell \le L \tag{5}$$

where $\tilde{u}_k = u_k\frac{\sin\beta}{\sin\alpha}$. $u_k = k\Delta$, *and* $\Delta = 2\pi\sin\alpha/T$. $\tilde{u} = u\frac{\sin\beta}{\sin\alpha}$. $u\in[0,\Delta]$. $\Theta_{\beta,\ell}(\cdot)$ *is the* β*th-order FrFT of* $\theta_\ell(\cdot)$.

According to αth-order FrFT, the semi-discrete convolution theorem and the Parseval's identity. The specific proof is as reference [5], [7].

Proof: Let $x(t)\in\mathcal{V}_{\alpha,\beta}(\theta_1,\cdots,\theta_L)$. Hence

$$x(t) = \sum_{\ell=1}^{L}\sum_{k=-\infty}^{+\infty} \varphi_\beta \lambda_\alpha^*(t)\hat{c}_{\alpha,\ell}[kT]\hat{\theta}_{\beta,\ell}(t-kT). \tag{6}$$

According to αth-order FrFT and the semi-discrete convolution theorem, the αth-order FrFT of $x(t)$ is as follows:

$$\begin{aligned}
X_\alpha(u) &= \int_{\mathbb{R}} x(t)K_\alpha(u,t)\mathrm{d}t \\
&= \varphi_\alpha\varphi_\beta \sum_{\ell=1}^{L}\sum_{k\in\mathbb{R}} \hat{c}_{\alpha,\ell}[kT]\lambda_\alpha(u)e^{jkT\tilde{u}\csc\beta} \\
&\quad\times \int_{\mathbb{R}} \hat{\theta}_{\beta,\ell}(t-kT)e^{j(t-kT)\tilde{u}\csc\beta}\mathrm{d}t \\
&= \varphi_\alpha \sum_{\ell=1}^{L}\sum_{k\in\mathbb{R}} \hat{c}_{\alpha,\ell}[kT]\lambda_\alpha(u)e^{jkTu\csc\alpha}\lambda_\beta^*(\tilde{u})\Theta_{\beta,\ell}(\tilde{u}) \\
&= \sum_{\ell=1}^{L}\lambda_\beta^*(\tilde{u})C_{\alpha,\ell}(u)\Theta_{\beta,\ell}(\tilde{u})
\end{aligned} \tag{7}$$

where $C_{\alpha,\ell}(u)$ is the αth-order semi-discrete FrFT of $c_\ell(\cdot)$. $\Theta_{\beta,\ell}(\tilde{u})$ is the βth-order FrFT of $\theta_\ell(\cdot)$. $C_{\alpha,\ell}(u) = \varphi_\alpha\sum_{k=-\infty}^{+\infty} c_\ell(kT)\lambda_\alpha(u)\lambda_\alpha(kT)e^{-j\csc\alpha kTu}$.

$$\begin{aligned}
&\|\mathcal{X}_\alpha(u)\|_{L^2(\mathbb{R})}^2 \\
&= \int_{-\infty}^{+\infty}\sum_{\ell=1}^{L}\left|\lambda_\beta^*(\tilde{u})C_{\alpha,\ell}(u)\Theta_{\beta,\ell}(\tilde{u})\right|\mathrm{d}u \\
&= \sum_{\ell=1}^{L}\sum_{k=-\infty}^{+\infty}\int_{u_k}^{u_{k+1}} \left|C_{\alpha,\ell}(u)\Theta_{\beta,\ell}(\tilde{u})\right|^2\mathrm{d}u \\
&= \sum_{\ell=1}^{L}\sum_{k=-\infty}^{+\infty}\int_0^{\Delta} \left|C_{\alpha,\ell}(u+u_k)\right|^2\left|\Theta_{\beta,\ell}(\tilde{u}+\tilde{u}_k)\right|^2\mathrm{d}u
\end{aligned} \tag{8}$$

Since $e^{-j\csc\alpha nTu_k} = e^{-2\pi nkj} = 1$, then:

$$\begin{aligned}
&C_{\alpha,\ell}(u+u_k) \\
&= \varphi_\alpha \sum_{n=-\infty}^{+\infty} Tc_\ell(nT)\lambda_\alpha(u+u_k) \\
&\quad\times\lambda_\alpha(nT)e^{-jnT(u+u_k)\csc\alpha} \\
&= \varphi_\alpha \sum_{n=-\infty}^{+\infty} Tc_\ell(nT)\lambda_\alpha(u)\lambda_\alpha(nT)e^{-jnTu\csc\alpha} \\
&\quad\times\lambda_\alpha(u_k)e^{juu_k\cot\alpha}e^{-jnTu_k\csc\alpha} \\
&= C_{\alpha,\ell}(u)\lambda_\alpha(u+u_k)\lambda_\alpha^*(u).
\end{aligned} \tag{9}$$

Hence $\left|C_{\alpha,\ell}(u+u_k)\right| = \left|C_{\alpha,\ell}(u)\right|$, it follows that

$$\begin{aligned}
\|\mathcal{X}_\alpha(u)\|^2 &= \sum_{\ell=1}^{L}\sum_{k=-\infty}^{+\infty}\int_0^{\Delta}\left|C_{\alpha,\ell}(u)\right|^2\left|\Theta_{\beta,\ell}(\tilde{u})\right|^2\mathrm{d}u \\
&= \sum_{\ell=1}^{L}\int_0^{\Delta}\left|C_{\alpha,\ell}(u)\right|^2 G_{\beta,\Theta_\ell}(\tilde{u})\mathrm{d}u
\end{aligned} \tag{10}$$

where $G_{\beta,\Theta_\ell}(\tilde{u}) = \sum_{k=-\infty}^{+\infty}\left|\Theta_{\beta,\ell}(\tilde{u}+\tilde{u}_k)\right|^2$ is shifted Grammian of θ_ℓ with angle β.

According to the Parseval's identity.

$$\begin{aligned}
&\left\|C_{\alpha,\ell}(u)\right\|_{L^2(0,\Delta)}^2 \\
&= \int_0^{\Delta}\Bigg(\sum_{k,n=-\infty}^{+\infty} Tc_\ell(kT)K_\alpha(kT,u) \\
&\qquad\times Tc_\ell^*(nT)K_{-\alpha}(nT,u)\Bigg)\mathrm{d}u \\
&= |\varphi_\alpha|^2T^2\sum_{k,n=-\infty}^{+\infty} c_\ell(kT)c_\ell^*(nT)\lambda_\alpha(kT)\lambda_\alpha^*(nT) \\
&\quad\times\int_0^{\Delta} e^{j\csc\alpha u(n-k)T}\mathrm{d}u \\
&= |\varphi_\alpha|^2T\Delta\sum_{k=-\infty}^{\infty}|c_\ell(kT)|^2 \\
&= \sum_{k=-\infty}^{\infty}|c_\ell(kT)\lambda_\alpha(kT)|^2 = \|c_\ell(kT)\|^2.
\end{aligned} \tag{11}$$

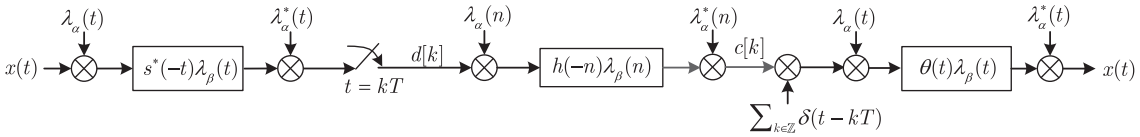

FIGURE 2. Single generator non-ideal sampling model in the SISs associated with the FrFT.

Because $|\varphi_\alpha|^2 = \varphi_\alpha\varphi_\alpha^* = \varphi_\alpha\varphi_{-\alpha} = \frac{1}{2\pi\sin\alpha}$, then $\Delta|\varphi_\alpha|^2 = \frac{1}{T}$. Thus

$$\|\mathcal{X}_\alpha(u)\|^2 = \sum_{\ell=1}^{L}\int_0^\Delta \left|C_{\alpha,\ell}(u)\right|^2 G_{\beta,\Theta_\ell}(\tilde{u})\mathrm{d}u. \tag{12}$$

Suppose $\zeta_1 \le G_{\beta,\Theta_\ell}(\tilde{u}) \le \zeta_2$, for $1 \le \ell \le L$, we have

$$\begin{aligned}\zeta_1\sum_{\ell=1}^{L}\|c_\ell(n)\|^2 &= \zeta_1\sum_{\ell=1}^{L}\|c_\ell(n)\lambda_\alpha(nT)\|^2\\ &\le \|x\|^2 \le \zeta_2\sum_{\ell=1}^{L}\|c_\ell(nT)\|^2\\ &= \zeta_2\sum_{\ell=1}^{L}\|c_\ell(nT)\lambda_\alpha(nT)\|^2.\end{aligned} \tag{13}$$

$\{\theta_\ell(t)\lambda_\beta(t)\}$ is a Riesz basis. This completes the proof of Theorem. 1. ■

B. NON-IDEAL SAMPLING MODELS

Let $\{\theta_\ell(t)\} \in L^2(\mathbb{R})$ be a compactly supported function whose infinite linear shifts span a subspace:

$$V_{\alpha,\beta}(\theta_1,\cdots,\theta_L) = \overline{\mathrm{span}}\sum_{\ell=1}^{L}\sum_{k=-\infty}^{+\infty}\hat{c}_{\alpha,\ell}(kT)\hat{\theta}_{\beta,\ell}(t-kT) \tag{14}$$

The scheme of the non-ideal sampling in the SISs associated with the FrFT is as Fig. 1.

$$\begin{aligned}d_\ell(t) &= \lambda_\alpha^*(t)\sum_{k=-\infty}^{+\infty}\hat{x}_\alpha(t)\hat{s}_{\beta,\ell}(t-kT)\\ D_{\alpha,\ell}(u) &= \varphi_\beta^{-1}\lambda_\beta^*(\tilde{u})X_\alpha(u)S_{\beta,\ell}^*(\tilde{u}),\end{aligned} \tag{15}$$

where $\tilde{u} = u\frac{\sin\beta}{\sin\alpha}$. $S_{\beta,\ell}(\tilde{u})$ is the βth-order FrFT of $s_\ell(t)$. Since $x(t) \in V_{\alpha,\beta}(\theta_1,\cdots,\theta_L)$, the αth-order FrFT of $x(t)$ is denoted by:

$$X_\alpha(u) = \mathcal{F}^\alpha(x)(u) = \sum_{\ell=1}^{L}\lambda_\beta^*(\tilde{u})C_{\alpha,\ell}(u)\Theta_{\beta,\ell}(\tilde{u}). \tag{16}$$

Substituting Eq. (16) into Eq. (15), we have

$$\begin{aligned}&D_{\alpha,\ell}(u)\\ &= \varphi_\beta^{-1}\sum_{k=-\infty}^{+\infty}\lambda_\beta^*(\tilde{u}-\tilde{u}_k)S_{\beta,\ell}^*(\tilde{u}-\tilde{u}_k)X_\alpha(u-u_k)\\ &= \varphi_\beta^{-1}\sum_{i=1}^{L}\lambda_\beta^*(\tilde{u})C_{\alpha,i}(u)\\ &\quad\times\sum_{k=-\infty}^{+\infty}\lambda_\beta^*(\tilde{u}-\tilde{u}_k)S_{\beta,\ell}^*(\tilde{u}-\tilde{u}_k)\Theta_{\beta,i}(\tilde{u}-\tilde{u}_k).\end{aligned} \tag{17}$$

Let $\Xi_{S\Theta}(u)$ as follows:

$$\Xi_{S\Theta}(u) = \begin{bmatrix}\xi_{S_{\beta,1}\Theta_{\beta,1}} & \cdots & \xi_{S_{\beta,1}\Theta_{\beta,L}}\\ \vdots & \vdots & \vdots\\ \xi_{S_{\beta,L}\Theta_{\beta,1}} & \cdots & \xi_{S_{\beta,L}\Theta_{\beta,L}}\end{bmatrix} \tag{18}$$

where $\xi_{S_{\beta,\ell}(u)\Theta_{\alpha,\ell}}(u) = \lambda_\beta^*(u)S_{\beta,\ell}^*(\tilde{u})\lambda_\beta^*(u)\Theta_{\beta,\ell}(u)$.

Then we have

$$\mathbf{D}_\alpha(u) = \varphi_\beta^{-1}\lambda_\beta^*(\tilde{u})\Xi_{S\Theta}(\tilde{u})\mathbf{C}_\alpha(u), \tag{19}$$

where $\mathbf{D}_\alpha(u) = [D_{\alpha,1}(u),\cdots,D_{\alpha,L}(u)]^T$. $\mathbf{C}_\alpha(u) = [C_{\alpha,1}(u),\cdots,C_{\alpha,L}(u)]^T$. Thus

$$\mathbf{C}_\alpha(u) = \varphi_\beta\lambda_\beta(\tilde{u})\Xi_{S\Theta}^{-1}(\tilde{u})\mathbf{D}_\alpha(u). \tag{20}$$

Substituting Eq. (15) into Eq. (20), the relationship between $x(t)$ and $\mathbf{C}_\alpha(u)$ is as follows:

$$\mathbf{C}_\alpha(u) = \Xi_{S\Theta}^{-1}(\tilde{u})X_\alpha(u)\mathbf{S}_\beta^*(\tilde{u}) = \mathbf{V}_\beta(\tilde{u})X_\alpha(u) \tag{21}$$

where $\mathbf{V}_\beta(\tilde{u}) = \Xi_{S\Theta}^{-1}(\tilde{u})\mathbf{S}_\beta^*(\tilde{u})$. $\mathbf{V}_\beta(\tilde{u})$ and $\mathbf{S}_\beta^*(\tilde{u})$ are the vectors with ℓth elements of $V_{\beta,\ell}(\tilde{u})$ and $S_{\beta,\ell}^*(\tilde{u})$ respectively. The time domain expression is as follows:

$$c_\ell(t) = \lambda_\alpha^*(t)\sum_{k=-\infty}^{+\infty}\hat{x}_\alpha(t)\hat{v}_{\beta,\ell}(t-kT). \tag{22}$$

where $1 \le \ell \le L, n \in \mathbb{Z}$. The βth-order FrFT of $v_\ell(t)$ is $V_{\beta,\ell}(u)$.

The function set $\{v_\ell(t-nT)\}$ is orthogonal to $\{\theta_\ell(t)\}$, The proof is as follows:

Proof:

$$\begin{aligned}&[\Xi_{V\Theta}(\tilde{u}]_{i\ell}\\ &= \frac{1}{T}\sum_{k\in\mathbb{Z}}V_{\beta,i}^*\left(\tilde{u}-\frac{2\pi\sin\beta}{T\sin\alpha}k\right)\Theta_\ell\left(\tilde{u}-\frac{2\pi\sin\beta}{T\sin\alpha}k\right)\\ &= \frac{1}{T}\sum_{r=1}^{L}[\Xi_{S\Theta}^{-1}(\tilde{u})]_{ir}\sum_{k\in\mathbb{Z}}S_r^*\left(\tilde{u}-\frac{2\pi\sin\beta}{T\sin\alpha}k\right)\\ &\quad\times\Theta_\ell\left(\tilde{u}-\frac{2\pi\sin\beta}{T\sin\alpha}k\right)\\ &= [\Xi_{S\Theta}^{-1}(\tilde{u})]^i[\Xi_{S\Theta}(\tilde{u})]_\ell = \mathbf{I}_{i\ell}\end{aligned} \tag{23}$$

where $[\mathbf{J}]_i$ denotes the ith row and $[\mathbf{J}]^i$ denotes the ith column respectively of the matrix $\mathbf{J}$.

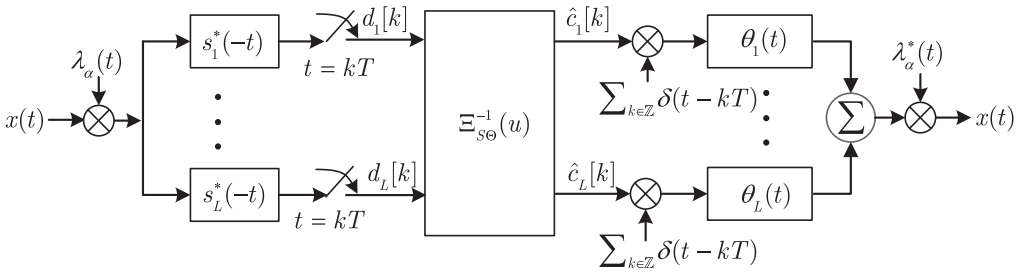

FIGURE 3. Simplified non-ideal sampling model with multiple generators in the SISs associated with the FrFT.

This follows that $[\Xi_{V\Theta}(u\csc\alpha)] = \mathbf{I}$. Thus, $\{v_\ell(t-nT)\}$ are orthogonal to $\{\theta_\ell(t)\}$. ■

Eq. (21) can be used to recover $x(t)$ from the sampled value as long as $\Xi_{S\Theta}(u)$ is invertible. The scheme of Fig. 1 results in L sequences of samples, each at rate $\frac{2\pi}{T}$, and the total sampling rate $\frac{2\pi L}{T}$. Sampling in $\mathcal{V}_{\alpha,\beta}(\theta_1,\cdots,\theta_L)$ is a suitable and realistic model for a variety of real application, such as, real acquisition and reconstruction devices, numerical implementation. These requirements can often be met by choosing appropriate generator $\{\theta_\ell\}$ of $\mathcal{V}_{\alpha,\beta}(\theta_1,\cdots,\theta_L)$.

Suppose that $L = 1$, Theorem 1 reduces to follows:

Corollary 1 (Single Generator SISs Associated With the FrFT): let $c(\cdot) \in \ell^2$, $\theta(\cdot) \in L^2(\mathbb{R})$ and consider the chirp-modulated SISs of $L^2(\mathbb{R})$.

$$\mathcal{V}_{\alpha,\beta}(\theta) = \left\{x(t) = \varphi_\beta\lambda_\alpha^*(t)\sum_{k=-\infty}^{+\infty}\hat{c}_\alpha[kT]\hat{\theta}_\beta(t-kT)\right\} \quad (24)$$

where $\hat{\theta}_\beta(t-kT) = \lambda_\beta(t-kT)\theta(t-kT)$, $\hat{c}_\alpha(kT) = \lambda_\alpha(kT)c(kT)$.

$\hat{\theta}_\beta(\cdot)$ is a Riesz basis for $\mathcal{V}_{\alpha,\beta}(\theta)$ if and only if there exist two positive constants $\zeta_1, \zeta_2 > 0$ such that:

$$\zeta_1 \le \sum_{k=-\infty}^{+\infty}\left\|\Theta_\beta(\tilde{u}-\tilde{u}_k)\right\|^2 \le \zeta_2 \quad (25)$$

where $\tilde{u}_k = u_k\frac{\sin\beta}{\sin\alpha}$. $u_k = k\Delta$, and $\Delta = 2\pi\sin\alpha/T$. $\tilde{u} = u\frac{\sin\beta}{\sin\alpha}$. $u \in [0,\Delta]$. $\Theta_\beta(\cdot)$ is the βth-order FrFT of $\theta(\cdot)$.

The non-ideal scheme in the SISs with single generator as Eq. (24) is in Fig. 2. Let $c(\cdot) \in \ell^2$, $\theta(\cdot) \in L^2(\mathbb{R})$ and consider the chirp-modulated SISs of $L^2(\mathbb{R})$,

$$x(t) = \varphi_\beta\lambda_\alpha^*(t)\sum_{k=-\infty}^{+\infty}\hat{c}_\alpha[kT]\hat{\theta}_\beta(t-kT) \quad (26)$$

Suppose the digital filter in the FrFD is as follows:

$$\varphi_\beta\lambda_\beta(\tilde{u})H_\beta^{-1}(\tilde{u}) = \varphi_\beta^{-1}\lambda_\beta^*(\tilde{u})S_\beta^*(\tilde{u})\lambda_\beta^*(\tilde{u})\Theta_\beta(\tilde{u}) \quad (27)$$

where $H_\beta(\tilde{u})$ is the βth-order FrFT of $h(n)$. $x(t)$ can be perfectly recovered from this sampling scheme, since $C_\alpha(u) = \varphi_\beta^{-1}\lambda_\beta^*(\tilde{u})D_\alpha(u)H_\beta(\tilde{u})$.

Suppose that $\beta = \alpha$ and $L = 1$, Theorem 1 reduces to traditional sampling method with single generator.

C. SIMPLIFIED NON-IDEAL SAMPLING MODEL

Suppose that $\beta = \frac{\pi}{2}$, Theorem 1 reduces to follows:

Corollary 2: let $\{c_\ell(\cdot)\} \in \ell^2$,$\{\theta_\ell(\cdot)\} \in L^2(\mathbb{R})$, $1 \le \ell \le L$ and consider the chirp-modulated SISs of $L^2(\mathbb{R})$.

$$\mathcal{V}_{\alpha,\frac{\pi}{2}}(\theta_1,\cdots,\theta_L) = \left\{x(t) = \frac{1}{\sqrt{2\pi}}\sum_{\ell=1}^{L}\lambda_\alpha^*(t)\sum_{k=-\infty}^{+\infty}\hat{c}_{\alpha,\ell}[kT]\theta_\ell(t-kT)\right\}, \quad (28)$$

where $\hat{c}_{\alpha,\ell}(kT) = \lambda_\alpha(kT)c_\ell(kT)$

Then $\{\theta_\ell(\cdot)\}$ is a Riesz basis for $\mathcal{V}_{\alpha,\frac{\pi}{2}}(\theta_1,\cdots,\theta_L)$ if and only if there exist two positive constants $\zeta_1, \zeta_2 > 0$ such that:

$$\zeta_1 \le \sum_{k=-\infty}^{+\infty}\|\Theta_\ell(\tilde{u}-\tilde{u}_k)\|^2 \le \zeta_2, \quad 1 \le \ell \le L, \quad (29)$$

where $\tilde{u}_k = u_k\csc\alpha$. $u_k = k\Delta$, and $\Delta = 2\pi\sin\alpha/T$. $\tilde{u} = u\csc\alpha$. $u \in [0,\Delta]$. $\Theta_\ell(\cdot)$ is the FT of $\theta_\ell(\cdot)$.

The non-ideal sampling method in $\mathcal{V}_{\alpha,\frac{\pi}{2}}(\theta_1,\cdots,\theta_L)$ is as Fig. 3. The non-ideal sampling model in Fig. 1 applied many chirp mixing which would increase the complexity of hardware design and energy consuming. Compared with Fig. 1, Fig. 3 is a simplified sampling structure. Considering $x(t) \in \mathcal{V}_{\alpha,\frac{\pi}{2}}(\theta_1,\cdots,\theta_L)$.

$$x(t) = \frac{1}{\sqrt{2\pi}}\sum_{\ell=1}^{L}\sum_{k=-\infty}^{+\infty}\lambda_\alpha^*(t)\hat{c}_{\alpha,\ell}(kT)\theta_\ell(t-kT) \quad (30)$$

The αth-order FrFT of $x(t)$ is denoted by:

$$\begin{aligned}X_\alpha(u) &= \mathcal{F}^\alpha(x)(u)\\ &= \frac{1}{\sqrt{2\pi}}\mathcal{F}^\alpha\left\{\sum_{\ell=1}^{L}\sum_{k=-\infty}^{+\infty}\lambda_\alpha^*(t)\hat{c}_{\alpha,\ell}(kT)\theta_\ell(t-kT)\right\}(u)\\ &= \mathscr{F}\left\{\sum_{\ell=1}^{L}\sum_{k=-\infty}^{+\infty}\hat{c}_{\alpha,\ell}(kT)\theta_\ell(t-kT)\right\}(u\csc\alpha)\\ &= \varphi_\alpha\sum_{\ell=1}^{L}\hat{C}_\ell(u\csc\alpha)\Theta_\ell(u\csc\alpha)\\ &= \varphi_\alpha\sum_{\ell=1}^{L}\Theta_\ell(u\csc\alpha)\int_{-\infty}^{\infty}\lambda_\alpha(t)e^{ju\csc\alpha t}c_\ell(t)\mathrm{d}t\end{aligned}$$

$$= \sum_{\ell=1}^{L} \lambda_\alpha^*(u) C_{\alpha,\ell}(u) \Theta_\ell(u \csc\alpha) \tag{31}$$

where $\mathscr{F}$ is the Fourier transform (FT) operator.

According to Fig. 3, $d_\ell(t)$ is denoted by:

$$d_\ell(t) = \sum_{k=-\infty}^{+\infty} \hat{x}_\alpha(t) s_\ell^*(t - kT)$$

$$D_\ell(u \csc\alpha) = \frac{1}{\sqrt{2\pi}} \varphi_\alpha^{-1} \lambda_\alpha^*(u) X_\alpha(u) S_\ell^*(u \csc\alpha), \tag{32}$$

where $S_\ell^*(u \csc\alpha)$ is the FT of $s_\ell(t)$.

Substituting Eq. (31) into Eq. (32), we have

$$\begin{aligned} &D_\ell(u \csc\alpha) \\ &= \frac{1}{\sqrt{2\pi}} \varphi_\alpha^{-1} \sum_{k=-\infty}^{+\infty} \lambda_\alpha^*(u - u_k) S_\ell^* \left(\frac{u - u_k}{\sin\alpha} \right) X_\alpha(u - u_k) \\ &= \frac{1}{\sqrt{2\pi}} \varphi_\alpha^{-1} \sum_{i=1}^{L} \lambda_\alpha^*(u) C_{\alpha,i}(u) \\ &\quad \times \sum_{k=-\infty}^{+\infty} \lambda_\alpha^*(u - u_k) S_\ell^* \left(\frac{u - u_k}{\sin\alpha} \right) \Theta_i \left(\frac{u - u_k}{\sin\alpha} \right). \end{aligned} \tag{33}$$

Let $\Xi_{S\Theta}(u \csc\alpha)$ as:

$$\Xi_{S\Theta}(u \csc\alpha) = \begin{bmatrix} \xi_{S_1\Theta_1} & \cdots & \xi_{S_1\Theta_L} \\ \vdots & \vdots & \vdots \\ \xi_{S_L\Theta_1} & \cdots & \xi_{S_L\Theta_L} \end{bmatrix} \tag{34}$$

where $\xi_{S_\ell\Theta_i} = S_\ell^*(u \csc\alpha)\Theta_i(u \csc\alpha)$.

Eq. (33) simplifies as follows:

$$\mathbf{D}(u \csc\alpha) = \frac{1}{\sqrt{2\pi}} \varphi_\alpha^{-1} \lambda_\alpha^*(u) \Xi_{S\Theta}(u \csc\alpha) \mathbf{C}_\alpha(u), \tag{35}$$

where $\mathbf{D}(u \csc\alpha) = [D_1(u \csc\alpha), \cdots, D_L(u \csc\alpha)]^T$. $\mathbf{C}_\alpha(u) = [C_{\alpha,1}(u), \cdots, C_{\alpha,L}(u)]^T$. Thus

$$\mathbf{C}_\alpha(u) = \sqrt{2\pi} \varphi_\alpha \lambda_\alpha(u) \Xi_{S\Theta}^{-1}(u \csc\alpha) \mathbf{D}(u \csc\alpha). \tag{36}$$

According to Eq. (32) and Eq. (36), the relationship between $x(t)$ and $\mathbf{C}_\alpha(u)$ is as:

$$\begin{aligned} \mathbf{C}_\alpha(u) &= \Xi_{S\Theta}^{-1}(u \csc\alpha) X_\alpha(u) \mathbf{S}^*(u \csc\alpha) \\ &= \mathbf{V}(u \csc\alpha) X_\alpha(u) \end{aligned} \tag{37}$$

where $\mathbf{V}(u \csc\alpha) = \Xi_{S\Theta}^{-1}(u \csc\alpha)\mathbf{S}^*(u \csc\alpha)$. $\mathbf{V}(u \csc\alpha)$ and $\mathbf{S}^*(u \csc\alpha)$ are the vectors with ℓth elements $V_\ell(u \csc\alpha)$ $S_\ell(u \csc\alpha)$ respectively. The time domain expression is as:

$$\begin{aligned} \hat{c}_{\alpha,\ell}(n) &= x(t) \otimes v_\ell(-t) \\ &= \int_{t=-\infty}^{\infty} v_\ell(t - nT) x(t) \mathrm{d}t \end{aligned} \tag{38}$$

where $1 \le \ell \le L, n \in \mathbb{Z}$. The FT of $v_\ell(t)$ is $V_\ell(u)$.

The function set $\{v_\ell(t - nT)\}$ is orthogonal to $\{\theta_\ell(t)\}$, the proof is similar to Eq. (23).

Eq. (36) can be used to recover $x(t)$ from L sampling sequence as long as $\Xi_{S\Theta}(u \csc\alpha)$ is invertible. The non-ideal sampling model of Fig. 3 explicitly how to recover $x(t)$ from these samples by an appropriate filter bank. The scheme results in m sequences of samples, each at rate $\frac{2\pi}{T}$, and overall sampling rate is $\frac{2\pi L}{T}$.

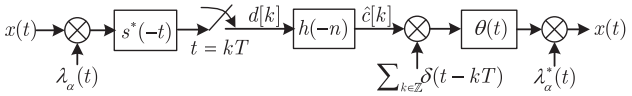

FIGURE 4. Simplified non-ideal sampling model with single generator in the SISs associated with the FrFT.

Suppose that $\beta = \frac{\pi}{2}$, $L = 1$, Theorem 1 reduces to the follows:

Corollary 3: let $c(\cdot) \in \ell^2$. $\theta(\cdot)$ is a continuous function in $L^2(\mathbb{R})$. The space $\mathcal{V}_{\alpha,\frac{\pi}{2}}(\theta)$ is a well-defined, closed subspace of $L^2(\mathbb{R})$ with Riesz basis $\{\theta(t - nT)\lambda_\alpha^*(t)\lambda_\alpha(nT)\}_{n\in\mathbb{Z}}$ if and only if there exist two positive constants $0 < \zeta_1 \le \zeta_2 < +\infty$, such that [12]

$$\zeta_1 \le 2\pi G_\Theta(u \csc\alpha) \le \zeta_2, u \in \mathbb{R} \tag{39}$$

where $G_\Theta(u \csc\alpha)$ is defined as:

$$G_\theta(u \csc\alpha) \triangleq \sum_{k\in\mathbb{Z}} |\Theta(u \csc\alpha + 2k\pi)|^2 \tag{40}$$

Based on the above facts, Shi *et al.* [12] gave the sampling theorem for the FrFT without bandlimited constraints. A simplified non-ideal sampling scheme in the SISs with single generator for Fig. 2 is as Fig. 4. The simplified sampling method for single channel would reduce hardware design and energy consuming. This simplified structure is derived from the Corollary 3. Suppose the digital filter $h(n)$ is such that:

$$H(u \csc\alpha) = \frac{\sqrt{2\pi}\varphi_\alpha \lambda_\alpha(u)}{S^*(u \csc\alpha)\Theta(u \csc\alpha)} \tag{41}$$

where $H(u \csc\alpha)$ is the FT of the $h[n]$. $x(t)$ could be perfectly recovered by this sampling scheme, because $\hat{c}(t) = d(t) \otimes h(t)$. $\mathscr{F}(\hat{c})(u \csc\alpha) = \hat{C}(u \csc\alpha) = D(u \csc\alpha)H(u \csc\alpha)$. $D(u \csc\alpha)$ is the FT of $d(t)$.

Compared with the simplified non-ideal sampling schemes which only need two chirp mixings, the non-ideal sampling schemes in Fig. 1 and Fig. 2 need many chirp modulators which would increase the complexity of the hardware and energy consumption. Both the non-simplified and simplified schemes use the properties of the convolution, and the difference lies in the analysis methods: the non-simplified structure is analyzed by the FrFT, whereas the simplified method is analyzed by the FT. From the theoretical analysis, the simplified schemes simply reduce the complexity of the hardware design without improving the accuracy of recovered signal. The sampled signal in the simplified model is $x(t)\lambda_\alpha(t)$ instead of $x(t)$, correspondingly, the recovery process is the same with the sampling process. For some chirp-modulated signals, the simplified sampling method would reduce the complexity of the sampled value without changing the recovery accuracy.

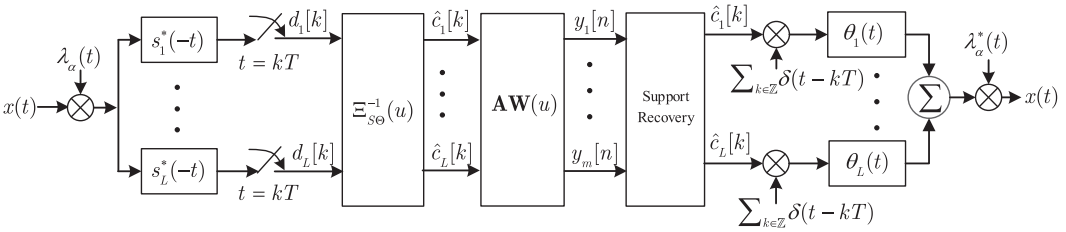

FIGURE 5. Compressed sampling associated with the SISs.

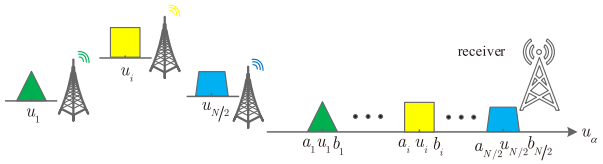

FIGURE 6. The multiband signal in the FrFD.

D. POTENTIAL APPLICATIONS

The proposed theory of generalized sampling spaces states that signals can be restored in summation of multiple generators in time domain. In other words, each signal can be expressed by the summation of several generators with different coefficients.

The applications of the proposed theorem can be found in processing some multiband signal whose energy is concentrated in the FrFD with several separated bandlimited components (see Fig. 6). These multiband signal is projected to the traditional one generator sampling space in which the sampling kernel must model the whole signal, but if each bandlimited component of multiband signal can be represented by one generator, and all the generators exist in different sampling channels, then the original signal can be expressed by the summation of several generators with different coefficients, each generator could be sampled by a relative low sampling rate.

Another example is chirp ultra-wideband signal which transmitted in some radar, sonar and communication system occupy very wide band which probably reach giga-hertz, thus designing a single channel sampling system with a flat spectrum in the whole band of signal is not practical, and multi-channel sampling architectures as reference [22]–[24] with each channel operating at a fractional of the Nyquist rate need to be employed. The multi-channel method applies multiple linear fractional filtering operators to represent bandlimited signal in the FrFD.

III. COMPRESSED SAMPLING IN THE SISs ASSOCIATED WITH THE FrFT

Theorem. 1 and its non-ideal sampling model point out that any signal $x(t)$ in generalized SISs generated by L functions shifted with period T can be perfectly recovered from L sampling sequences, which obtained by filtering $x(t)$ with a bank of filters and uniformly sampling with rate $\frac{2\pi}{T}$. The overall sampling rate is $\frac{2L\pi}{T}$. If the signal is generated by K out of L generators. The signal can be sampled at $\frac{2K\pi}{T}$ rate with uniform sampling rate $\frac{2\pi}{T}$ and K filters. Furthermore, how we can use a lower sampling rate when we know the signal is composed by K of the generators, but we do not know which generators. At this case, we can also recover signal from the original system with sampling the output of L filters, but it will result in the increasing of the sampling rate, and a waste of hardware. According to [24,25], there is a unique SI signal recovered from samples when the overall sampling rare is at least $\frac{2K\pi}{T}$. In follows, we will give an algorithm to recover $x(t)$ from sampling the output of $K \le m < L$ filters at sampling rate $1/T$.

In this part, we proposed two compressed sampling methods combining the ideas of CS and sampling in the SISs. The first method constructs a discrete CS algorithm which using the sensing matrix $\mathbf{A}$ to compressed the results of the sampling in the SISs. The second method realized by constructing random filters can be used to sample analog sparse signals directly in the FrFD, and the random filters consist of sensing matrix and the filter of SI sampling.

A. CS ASSOCIATED WITH THE SISs

Suppose the signal is generated by K out of L generators, then there are K out of L nonzero sequences $\hat{c}_\ell$ in Eq. (28). Under this assumption, the compressed sampling method for this situation is as Fig. 5. The approach combines analog front-end of Fig. 3 and discrete CS, consists of L filters and uniformly sample at rate $1/T$. Since the vector $\mathbf{C}[n]$ is sparse, we first use the infinite measurement vector model to recover the sparse vector $\mathbf{C}[n]$, then combine the results of Fig. 3 and the recovered sparse vector to reconstruct the original signal $x(t)$.

The vector sequence $\mathbf{C}[n]$ is an infinite vector which can be resolved by the infinite measurement vector model as:

$$\mathbf{y}[n] = \mathbf{A}\mathbf{c}[n], \quad n \in \mathbb{Z} \tag{42}$$

where the sensing matrix $\mathbf{A} \in \mathbb{Z}^{L\times m}$. $\mathbf{A}$ satisfies the restricted isometry property (RIP), that means K-sparse vector $\mathbf{C}[n]$ can be perfectly recovered from m measurement. Eq. (42) can be resolved by transforming it to an equivalent MMV. The recovery properties of equation depend on the matrix $\mathbf{A}$ [25]. The reconstruction algorithm is depicted by continuous-to-finite (CTF) [25].

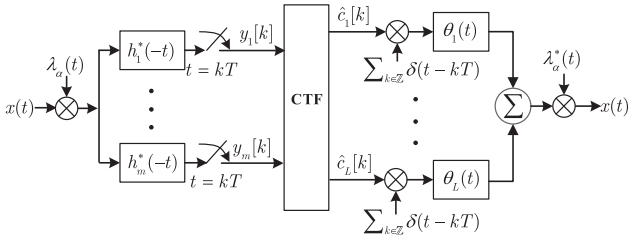

FIGURE 7. Compressed sampling analog associate with the SISs.

In our paper, we consider the generalized equation in the FrFD as:

$$\mathbf{Y}_\alpha(u) = \mathbf{W}(u)\mathbf{A}\mathbf{C}_\alpha(u) \tag{43}$$

where $\mathbf{Y}_\alpha(u)$, $\mathbf{C}_\alpha(u)$ are the vectors with components $Y_{\alpha,\ell}(u)$ and $C_{\alpha,\ell}(u)$. $\mathbf{W}(u)$ is an invertible $m\times m$ matrix with elements $W_{i\ell}(u)$. Eq. (43) expresses in time domain as:

$$y_i[n] = \sum_{\ell=1}^{m} w_{i\ell} \otimes \left(\sum_{r=1}^{L} A_{\ell r}\hat{c}_r[n]\right), \quad 1 \le i \le m \tag{44}$$

where $w_{i\ell}$ is the DFT of $W_{i\ell}(u)$. $\otimes$ denotes the convolution operator.

According to Eq. (43) and Eq. (44), we can recover the sequence $\hat{c}_\ell[n]$ from $m < L$ discrete time sequence $y[n]$ either in the FrFD or time domain. The drawback of the sampling scheme in Fig. 5 is obvious, that is the overall sampling rate is L/T which is not less than the traditional method, because the input signal must be fully sampled with L channels, then compressed by the CS matrix $\mathbf{A}$. In next section, we proposed a compressed sampling method of analog signal directly without discretization ahead.

B. CS OF ANALOG SIGNAL ASSOCIATED WITH SI

This approach consists of $m < L$ filters and uniformly sampling. Comparing with the fist method in the last section, CS of analog signal simplifies the design of hardware. The critical challenge is how to design the filters $\{h_\ell^*(t)\}$, $1 \le \ell \le m$ in the Fig. 7. A simple approach to design the filter bank is moving the discrete filters $\mathbf{\Xi}_{V\Theta}(u\csc\alpha)$ and sensing matrix $\mathbf{AW}(u)$ to the analog domain. The filters $\{h_\ell^*(t)\}$ combine the filters $\{s_\ell^*(t)\}$, the discrete filter $\mathbf{\Xi}_{V\Theta}(u\csc\alpha)$ and the sensing matrix $\mathbf{AW}(u)$. The compressed sampling results $y_\ell[n]$ can be obtained directly from $x(t)$ by uniformly sampling the output of p filters $\{h_\ell(t)\}$.

Let the filter bank $\mathbf{H}(u\csc\alpha)$ be constructed by:

$$\begin{aligned}\mathbf{H}(u\csc\alpha) &= \mathbf{W}^*(u\csc\alpha)\mathbf{A}^*\mathbf{V}(u\csc\alpha)\\ &= \mathbf{W}^*(u\csc\alpha)\mathbf{A}^*\mathbf{\Xi}_{S\Theta}^{-*}(u\csc\alpha)S(u\csc\alpha)\end{aligned} \tag{45}$$

where $\mathbf{H}(u\csc\alpha)$ is the vector with ℓth element $H_\ell(\cdot)$. $\mathbf{S}(u\csc\alpha)$ is the vector with ℓth element $S_\ell(\cdot)$. $\mathbf{V}(u\csc\alpha) = \mathbf{\Xi}_{S\Theta}^{-1}(u\csc\alpha)\mathbf{S}^*(u\csc\alpha)$. $\mathbf{V}(u\csc\alpha)$ is the vector with ℓth element $V_\ell(u\csc\alpha)$, which is the FT of $v_\ell(t)$. Eq. (45) in time domain is as follows:

$$h_i(t) = \sum_{\ell=1}^{m}\sum_{r=1}^{p}\sum_{n\in\mathbb{Z}} w_{ir}^*[-nT]A_{r\ell}^* v_\ell(t-nT) \tag{46}$$

where w_{ir} is the inverse FT of $[\mathbf{W}(u\csc\alpha)]_{ir}$.

$$v_i(t) = \sum_{\ell}^{m}\sum_{n\in\mathbb{Z}} \xi_{i\ell}^*[-nT]s_\ell(t-nT) \tag{47}$$

where $\xi_{i\ell}^*[-nT]$ is the inverse transform of $[\mathbf{\Xi}_{S\Theta}^{-1}(u\csc\alpha)]_{i\ell}$.

If we can proof the $\mathbf{\Xi}_{H\Theta}(u) = \mathbf{W}(u)\mathbf{A}$, then $x(t)$ can be perfectly recovered from m sampling sequence $\{y_\ell[n]\}$, which can be obtained by sampling the output of the filters $\{h_\ell^*(-t)\}$ at the rate $\frac{1}{T}$.

$$\begin{aligned}&[\mathbf{\Xi}_{H\Theta}(u)]_{i\ell}\\ &= \frac{1}{T}\sum_{k\in\mathbb{Z}} H_i^*\left(\frac{u}{\sin\alpha} - \frac{2k\pi}{T\sin\alpha}\right)\Theta_\ell\left(\frac{u}{\sin\alpha} - \frac{2k\pi}{T\sin\alpha}\right)\\ &= \frac{1}{T}\sum_{r=1}^{m}[\boldsymbol{W}(u)\boldsymbol{A}]_{ir}\sum_{k\in\mathbb{Z}} V_r^*\left(\frac{u}{\sin\alpha} - \frac{2k\pi}{T\sin\alpha}\right)\\ &\quad\times\Theta_\ell\left(\frac{u}{\sin\alpha} - \frac{2k\pi}{T\sin\alpha}\right)\\ &= [\mathbf{W}(u)\mathbf{A}]_i[\mathbf{\Xi}_{V\Theta}(u)]^\ell\end{aligned} \tag{48}$$

where $[\mathbf{J}]_i$ denotes the ith row and $[\mathbf{J}]^i$ denotes the ith column respectively of the matrix $\mathbf{J}$.

Since $[\mathbf{\Xi}_{V\Theta}(u)]$ is a $m\times m$ identity matrix in Eq. (23), the equation $\mathbf{\Xi}_{H\Theta}(u) = \mathbf{W}(u)\mathbf{A}$ is proved. From the foregoing analysis, scheme of Fig. 7 can be used to compressive sample analog signals directly. The compressed sampling scheme consists of filter band, uniformly sampling, CTF (continuous to finite) and a set of generators. The system can compressively and directly sample the analog signal by filtering $x(t)$ with $m < L$ filters. The coefficients of the generators are reconstructed by the CTF block. The signal can be finally reconstructed by linear combination of generators.

In this section, we first use the conventional theory of CS to sample and recover the sparse basis of signal in the SISs. Considering this proposed scheme is a discrete problem which cannot compressive sample directly, we proposed a compressed sampling method of analog signal associated with the SISs by constructing a bank of filters and uniformly sampling. This approach can be easy to put into practice.

IV. NUMERICAL SIMULATION

In many practical applications, sampling a chirp signal is ubiquitous in radar, sonar and communications systems [2]. The Nyquist sampling rate in the FrFD is lower than the conventional Fourier domain for sampling a chirp signal. We demonstrate the numerical simulation in two parts including multiple generators sampling method and compressed sampling in the SISs associated with the FrFT.

TABLE 1. Parameters of signal.

Parameters	Value	meaning
$\mathcal{N}$	2	number of chirp signals
E_1	1.5	Amplitude for component 1
k_1	2	Frequency modulated scale for component 1
f_1	20	Carrier frequency for component 1
E_2	2	Amplitude for component 2
k_2	3	Frequency modulated scale for component 2
f_2	-18	Carrier frequency for component 2

From the theoretical analysis, the difference between the non-simplified and simplified schemes is the analysis method. The simplified method sample and reconstruct signals in the traditional Fourier domain, whereas the non-simplified method is in the FrFD which needs more chirp modulators. The simplified schemes simply reduce the complexity of the hardware design without improving the accuracy of the recovered signal. The non-simplified and simplified methods have the same recovered waveform when sampling and reconstructing the same signals. For some chirp-modulated signals, the simplified sampling method would reduce the complexity of the sampled value but not change the recovery accuracy.

A. SAMPLING WITH MULTIPLE GENERATORS IN THE SISs

In this part, we consider a problem of sampling multiband signal which is a complex signal comprised by several bandlimited signal. The sampled mulbiband signal is given by:

$$x(t) = \sum_{i=1}^{\mathcal{N}} E_i \mathrm{rect}(t) \exp(-j\pi k_i t^2) \exp(\pi f_i t) \tag{49}$$

where rect$(\cdot)$ is a rectangle time-window.

The parameters in Eq. (49) is as table 1.

The fractional order of the FrFT is $\alpha = \mathrm{arccot}(k_1)$. The maximum fractional Fourier frequency is 21π, $t \in [-1, 1)$, so the bandwidth of the selected generator must be wider than the sampled signal's bandwidth. In order to compare with other methods, we demonstrate the simulation results for three different cases, including the traditional method with multiple generators, the single generator method associated with the FrFT and the proposed multiple generators method. The multiple generators for traditional sampling method are selected as $\{e^{-18j\pi t}\mathrm{sinc}(8t), e^{20j\pi t}\mathrm{sinc}(5t)\}$. The single generator is selected as $e^{j\cot\alpha t^2}\{\mathrm{sinc}(21t)\}$. The multiple generators for the proposed method are selected as $e^{j\cot\alpha t^2}\{e^{-18j\pi t}\mathrm{sinc}(8t), e^{20j\pi t}\mathrm{sinc}(5t)\}$. Using the normalized mean squared error (NMSE) to evaluate the performance of the sampling method. NMSE is denoted by:

$$\mathrm{NMSE} = \frac{\int_{-\infty}^{+\infty} |x(t) - \bar{x}(t)|^2 \mathrm{d}t}{\int_{-\infty}^{+\infty} |x(t)|^2 \mathrm{d}t} \tag{50}$$

where $x(t)$ is the original signal and $\bar{x}(t)$ denotes the recovered signal.

Fig. 8 shows the recovery accuracy with the different sampling rates and the SNR. The sampling rate ranges in {25, 50, 100}Hz. SNR ranges in [1,10] with step 1.

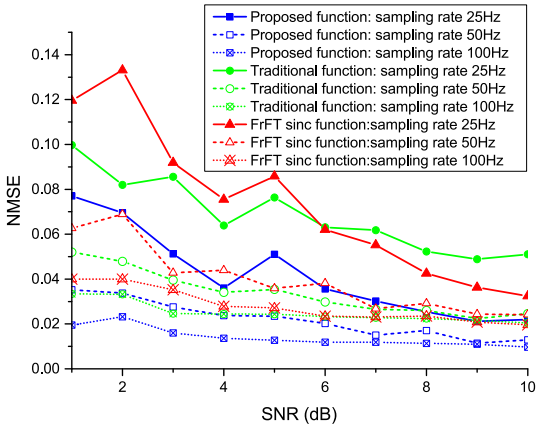

FIGURE 8. NMSE of the chirp signals with different sampling rates and SNRs.

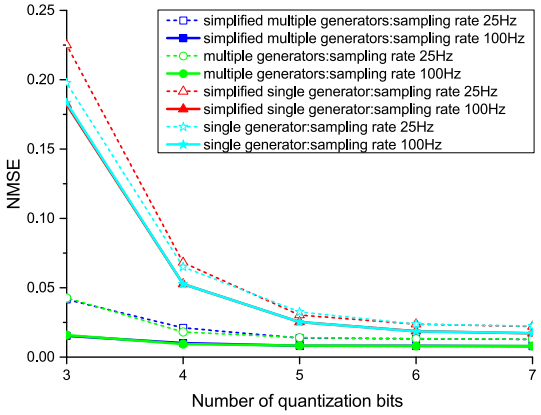

FIGURE 9. NMSE of the chirp signals with different sampling rates and quantization bits.

The recovery accuracy increases with the SNR and sampling rate increasing. It is obvious our proposed multiple generators method in Eq. (4) has higher recovery accuracy under the same sampling conditions.

Fig. 9 shows the recovery accuracy under the different sampling rate and number of sampling quantization bits. The sampling rate ranges in {25, 100}Hz. The number of sampling quantization bits is {3, 4, 5, 6, 7}. The recovery accuracy increases with the number of sampling quantization bits and the sampling rate increasing until the number of sampling quantization bits reaches 6. The traditional multiple generators method has higher recovery accuracy compared with single function method as Eq. (24). To reach the same recovery accuracy, the traditional methods need higher sampling rate. The simplified generators methods have the similar recovery accuracy under the same sampling condition for both multiple generators method and single generator methods. The multiple generator sampling methods have better recovery accuracy for the chirp type signal than the single generator methods.

In this part, the sampled signal is a typical multiband signal which is comprised by two bandlimited signals, the traditional method for this type signal must work at least twice

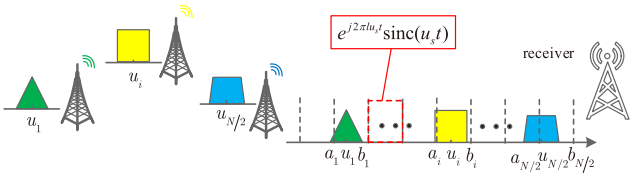

FIGURE 10. The multiband signal represented by multiple generators.

the maximum fractional Fourier frequency of the signal. The sampled signal can be efficiently modeled by the multiple generators, in which, every generator can use a low sampling rate model, thus, the high sampling rate is not necessary.

B. COMPRESSED SAMPLING FOR MULTI-BAND SIGNALS IN FrFD

In most applications, how to choose the generators in the SI sampling spaces is difficult. To simplify the design of compressed sampling method, we propose a multichannel parallel sampling and recovery architecture. The proposed method averages the whole sampling region into several equal intervals in the FrFD. The multiple generators are selected as:

$$\begin{aligned}&\{\theta_1,\cdots,\theta_\ell,\cdots,\theta_{L_0},\cdots,\theta_{2L_0+1}\}\\&\quad=\{e^{-j2\pi L_0 u_s t}\mathrm{sinc}(u_s t),\cdots,e^{-j2\pi\ell u_s t}\mathrm{sinc}(u_s t),\\&\qquad\cdots,\mathrm{sinc}(u_s t),e^{j2\pi u_s t}\mathrm{sinc}(u_s t),\\&\qquad\cdots,e^{j2\pi L_0 u_s t}\mathrm{sinc}(u_s t)\}\end{aligned}\tag{51}$$

where $L=2L_0+1$ is the number of generators. To cover the whole bandwidth, $L\geq(u_{NYQ}/u_s)$, where $u_{NYQ}/2$ is the maximum frequency in the FrFD. u_s is the bandwidth of the generator. The SI sampling subspaces which is comprised by the selected generator satisfies the condition Theorem 1. We select $\mathbf{\Xi}^{-*}_{S\Theta}(u\csc\alpha)=\mathbf{I}$ in Eq. (45), where $\mathbf{I}$ is an identity matrix. Since $\mathbf{\Xi}^{-*}_{S\Theta}(u\csc\alpha)=\mathbf{I}$, $\mathbf{S}^*(\cdot)$ and the generators $\mathbf{\Theta}(\cdot)$ are orthogonal, $\mathbf{S}^*(\cdot)$ is the same with the generators $\mathbf{\Theta}(\cdot)$. It's obvious every generator has the same bandwidth, and all generators average the whole sampled zone into L parts as Fig. 10.

The random sampling matrix $\mathbf{P}\in\{\pm1\}^{m\times N}$ is selected as a different periodic repeating pattern of M random equiprobable sign values, in which all of the elements are $\{\pm1\}$. $\mathbf{P}$ is a discrete sequence which is realized by:

$$p_i(t)=P_{ik},\ k\frac{T_p}{N}\leqslant t\leqslant(k+1)\frac{T_p}{N},\ 0\leqslant k\leqslant N-1\tag{52}$$

where $p_i(t)$ is the ith row of $\mathbf{P}$. $P_{ik}\in\{+1,-1\}$ and the period of $p_i(t)$ is T_p. The index $i=1,2,\cdots,m$ identifies the mixing channel. Sign vectors are assumed to be mutually uncorrelated with $E[p_i^T(t),p_j(t)]=0$ for $i\neq j$. $E[\cdot]$ denotes the statistical expectation operator which is referred to the probability of sign values. The Fourier expansion of T_p-periodic $p_i(t)$ and its coefficient c_{il} are as follows:

$$p_i(t)=\sum_{l=-\infty}^{+\infty}c_{il}e^{j\frac{2\pi}{T_p}lt},$$

$$c_{il}=\frac{1}{T_p}\int_0^{T_p}p_i(t)e^{-j\frac{2\pi}{T_p}lt}\mathrm{d}t.\tag{53}$$

$h_i(t)$ is the time expression which is denoted by:

$$\begin{aligned}&h_i(t)\\&\quad=\sum_{\ell=-L_0}^{L_0}\sum_{n\in\mathbb{Z}}p_i(nT)e^{j\ell u_s(t-nT)}\mathrm{sinc}(u_s(t-nT))\end{aligned}\tag{54}$$

According to Eq. (45), suppose $\mathbf{\Xi}^{-*}_{S\Theta}(u\csc\alpha)$ is an identity diagonal matrix.

$$\begin{aligned}H_i(u)&=\mathscr{F}\{p_i\}(u)\mathscr{F}\left\{\sum_{\ell=-L_0}^{L_0}e^{j2\pi\ell u_s t}\mathrm{sinc}(u_s t)\right\}(u)\\&=\int_{\mathbb{R}}\sum_{l=-\infty}^{+\infty}c_{il}e^{j\frac{2\pi}{T_p}lt}e^{-j2\pi ut}\mathrm{d}t\\&\quad\times\int_{\mathbb{R}}\sum_{\ell=-L_0}^{L_0}e^{j2\pi\ell u_s t}\mathrm{sinc}(u_s t)e^{-j2\pi ut}\mathrm{d}t\\&=\sum_{l=-\infty}^{+\infty}c_{il}\delta(u-\frac{l}{T_p})\sum_{\ell=-L_0}^{L_0}\mathrm{rect}((u-\ell)u_s)\end{aligned}\tag{55}$$

where $\mathrm{rect}(\cdot)$ is a rectangular window.

$x(t)$ is sent in parallel to m mixing channels simultaneously. Taking ith channel as an example, $x(t)$ is filtered by $h_i(t)$, the filtered result is as:

$$\begin{aligned}&x(t)\lambda_\alpha(t)\otimes h_i(t)\\&\quad=\int_{\mathbb{R}}x(\tau)\lambda_\alpha(\tau)h_i(t-\tau)\mathrm{d}\tau\\&\quad=\int_{\mathbb{R}}x(\tau)\lambda_\alpha(\tau)\sum_{\ell=-L_0}^{L_0}\sum_{n\in\mathbb{Z}}p_i(nT)e^{j\ell u_s(t-\tau-nT)}\\&\qquad\times\mathrm{sinc}(u_s(t-\tau-nT))\mathrm{d}\tau\end{aligned}\tag{56}$$

The FT of the filtered results is denoted by:

$$\begin{aligned}\mathcal{Y}_{\alpha,i}(u\csc\alpha)&=\mathscr{F}\left\{x(t)\lambda_\alpha(t)\otimes h_i(t)\right\}(u\csc\alpha)\\&=\mathscr{F}\{x(t)\lambda_\alpha(t)\}(u\csc\alpha)H_i(u\csc\alpha)\\&=\varphi_\alpha^{-1}\lambda_\alpha^*(u)\mathcal{X}_\alpha(u)\sum_{l=-\infty}^{+\infty}c_{il}\delta(u\csc\alpha-\frac{l}{T_p})\\&\quad\times\sum_{\ell=-L_0}^{L_0}\mathrm{rect}((u\csc\alpha-\ell)u_s)\\&=\varphi_\alpha^{-1}\sum_{l=-\infty}^{\infty}c_{il}\lambda_\alpha^*(u-u_A l)\mathcal{X}_\alpha(u-u_p l)\\&\quad\times\sum_{\ell=-L_0}^{L_0}\mathrm{rect}((u-\ell\sin\alpha)u_s).\end{aligned}\tag{57}$$

where $u_p=2\pi\sin\alpha/T_p=\sin\alpha f_p$. $\mathcal{X}_\alpha(u)$ is αth-order FrFT of $x(t)$. It is a bandlimited signal with the maximum bandwidth not exceeding B_α.

$\lambda_\alpha^*(u-u_pl)\mathcal{X}_\alpha(u-u_pl)$ is also a bandlimited signal with the maximum bandwidth B_α and a relatively u_pl shifting in the FrFD. The mixing product is filtered by a low-pass filter with cutoff $u_s/2$. T_s is the sampling period for every single channel, $u_s = f_s \sin\alpha = \frac{2\pi \sin\alpha}{T_s}$ is the sampling rate. Since the anti-aliasing filter rect(u) is an ideal rectangle function in FrFD. rect(u) $= 1$, $u \in [-\frac{1}{2}, \frac{1}{2}]$, otherwise rect($u$) $= 0$.

$$\mathcal{Y}_{\alpha,i}(u) = \varphi_\alpha^{-1} \sum_{l=-L_0}^{L_0} c_{il}\lambda_\alpha^*(u-u_pl)\mathcal{X}_\alpha(u-u_pl). \quad (58)$$

The spectrum of $\tilde{\mathcal{Y}}_{\alpha,i}(u)$ is the repetition of the spectrum of $\lambda_\alpha^*(u)\mathcal{X}_\alpha(u)$. L_0 is chosen as the smallest integer such that it must cover all nonzero spectrum slices of the $\mathcal{X}_\alpha(u)$. The exact value of L_0 is calculated by: $-\frac{u_s}{2} + (L_0+1)u_p \geq \frac{u_{NYQ}}{2}$, then $L_0 = \left[\frac{u_{NYQ}+u_s}{2u_p}\right] - 1$. $u_s = f_s \sin\alpha$ is the fractional sampling rate. $u_p = f_p \sin\alpha$ is the fractional "frequency" of the mixing signal $p_i(t)$. The fractional Nyquist sampling rate of α-bandlimited signal is $u_{NYQ} = 2b_{N/2}$ when the maximum fractional Fourier "frequency" of the signal is $b_{N/2}$. $L_0 = (b_{N/2}\csc\alpha + f_s)/(2f_p) - 1$. We choose the sign matrix signal $f_p \geq B_\alpha \csc\alpha$, and the sampling rate $f_s = f_p \geq B_\alpha \csc\alpha$. The number of spectrum slices is $L = 2L_0 + 1$.

The ith channel interpolation formula is as:

$$y_i(t) = \frac{1}{2\pi} \sum_{l=-L_0}^{L_0} \sum_{n=-\infty}^{+\infty} c_{il}x(nT_s)\lambda_\alpha(nT_s) \times \frac{\sin[(t-nT_s)u_s \csc\alpha]}{(t-nT_s)u_s \csc\alpha} e^{jlu_p \csc\alpha(t-nT_s)}. \quad (59)$$

According to Eq. (53), $c_{il} = w_l \sum_{k=0}^{M-1} p_{ik}q^{lk}$ where $q = e^{j2\pi/M}$. $w_l = \frac{1}{M}$, for $l = 0$, else $w_l = \frac{1-q^l}{2j\pi l}$. Let $\bar{F}$ be the $M \times M$ discrete Fourier transformation matrix and the ith column: $\bar{F}_i = \left[q^{0i}, q^{1i}, \ldots, q^{(M-1)i}\right]^T$, $i \in [0, M-1]$. Let $\mathbf{F} = [\bar{F}_{L_0}, \cdots, \bar{F}_{-L_0}]$ be $M \times L$ matrix. To guarantee no distortion of the original signal's spectrum, set $M = L$. Let $\mathbf{S}$ be the $m \times M$ sign matrix. $\mathbf{W} = diag(w_{L_0}, \ldots, w_{-L_0})$ is a $L \times L$ diagonal matrix. Substituting the above definitions to Eq. (58),

$$\mathbf{Y}_\alpha(u) = \mathbf{PFW}\mathbf{z}_\alpha(u), \quad (60)$$

where $\mathbf{z}_\alpha(u) = \mathbf{G}(u)\mathbf{V}_\alpha(u)$, $\mathbf{V}_\alpha(u) = [\mathcal{X}_\alpha(u - L_0u_p), \cdots, \mathcal{X}_\alpha(u), \cdots, \mathcal{X}_\alpha(u + L_0u_p)]^T$. $\mathbf{G}(u) = \text{diag}[g_{L_0}, \cdots, g_{-L_0}]$, where $g_l = \lambda_\alpha^*(u - u_pl)$. Rewrite Eq. (58) in discrete fractional Fourier domain as $\boldsymbol{y}_{\alpha,i}(n) = \sum_{l=-L_0}^{L_0} c_{il}\boldsymbol{z}_{\alpha,l}(n)$, where $\boldsymbol{z}_{\alpha,l}(n)$ is the sampling sequence of the lth spectrum slice of $\mathbf{z}_\alpha(u)$. c_{il} is the entries of sensing matrix $\mathbf{A} = \mathbf{PFW}$. The matrix $\mathbf{A}$ and sub-Nyquist downsampling stage is an important implementation of the sub-Nyquist sampling which allows compressive acquisition of sparse wideband signals at sub-Nyquist rates. $\mathbf{z}_\alpha(u)$ can be recovered from Eq. (60) by using the simultaneous orthogonal matching pursuit (SOMP), which is fast and easy to implement for engineers to construct signals in the simulations.

TABLE 2. Parameters of signal.

Parameters	Values	Meanings
$\mathcal{N}$	6	Number of active bands
E_1	0.3	Amplitude for component 1
τ_1	0	Time delay for component 1
s_1	2μs	Time scale for component 1
k_1	6×10^{13}	Frequency modulated rate for component 1
f_1	9.5GHz	Carrier frequency for component 1
E_2	0.5	Amplitude for component 2
τ_2	0	Time delay for component 2
s_2	2μs	Time scale for component 2
k_2	5.5×10^{13}	Frequency modulated rate for component 2
f_2	8GHz	Carrier frequency for component 2
E_3	0.6	Amplitude for component 3
τ_3	0	Time delay for component 3
s_3	2μs	Time scale for component 3
k_3	5.25×10^{13}	Frequency modulated rate for component 3
f_3	2GHz	Carrier frequency for component 3

We use the chirp signal as the test subject which is a typical fractional Fourier bandlimited signal. Chirp-like signals can be interpreted as the first order approximation of the polynomial frequency modulation signals. The normalized mean squared error (NMSE) and successful recovery probability are used to measure the performance of the compressed sampling. Successful recovery probability is defined as the ratio of the number of empirical successful reconstructions and total trials. Successful recovery is defined when the estimated support set is equal to the true support. Obviously, the greater the successful recovery probability is, the better the performance. We demonstrate the results for two cases: the performance of proposed system with different generators, robustness and recovery accuracy with different SNRs, sparsity and number of channels. Every simulation has 300 trials to ensure statistically stable results. The original multiband signal is given by follows:

$$x(t) = \sum_{i=1}^{\mathcal{N}/2} E_i \text{rect}(\frac{t-\tau_i}{s_i}) \cos(2\pi k_i t^2 + 2\pi f_i t) \quad (61)$$

where $\mathcal{N}/2$ is the number of signals. Suppose the symmetry of the real signal spectrum, $\mathcal{N}$ is the sparsity. E_i is the amplitude of signal which could be random or fixed. s_i is the time scale factor which determines the signal duration, in our simulation, s_i is fixed to be 2μs. τ_i is the time delay between different signals which is selected randomly. k_i is the signal modulation rate. f_i is frequency carrier in $[f_s, f_{NYQ}]$. f_{NYQ} is 10GHz. With $\alpha = -0.2 \times 10^{-13}$ order FrFT, the bandwidth of three components are $\{40, 20, 10\}$MHz respectively which are computed by $(k_i - \cot\alpha)s_i$, so he maximum bandwidth and the minimum bandwidth are $B_{\alpha,\max} = 40$MHz and $B_{\alpha,\min} = 10$MHz. The specific values of the parameters are as table 2.

From the foregoing analysis, we can see the choice of the generators is the basis of the proposed method, which directly decides the implementation structure of the hardware. In our proposed method, the generators are chosen to average the total sampling region in the FrFD, as a result the number of the generators is the most important factor. In the following, we use simulations to find how the different numbers of generators decide the performance of the proposed method.

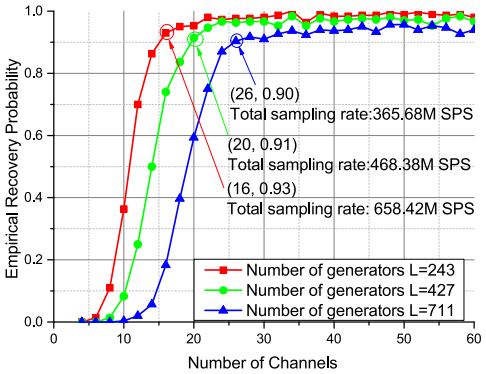

FIGURE 11. The recovery probability of the proposed method with different number of generators.

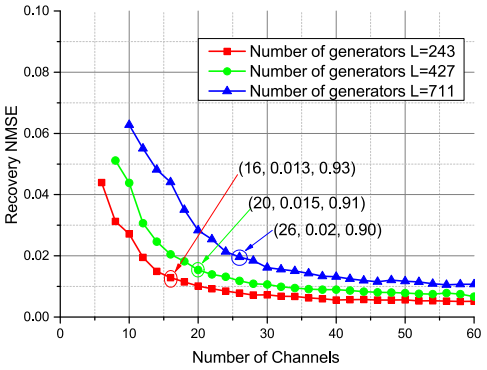

FIGURE 12. The recovery NMSE of the proposed method with different number of generators.

The simulation is evaluated by the recovery probability, accuracy and compressed ratio where the compressed ratio is computed by mu_s/u_{NYQ}, u_s is the width of the sperate grid, m is the number of channels.

Considering the maximum and minimum bandwidth of the sampled signals are 40MHz and 10MHz respectively, we use three representative number of generators {235, 463, 711}, as a result, the bandwidth of the three different types generators are {42.55, 21.6, 14.06}MHz. The three simulations can be used to simulate two situations, which shows the basic change trend of the performance with different bandwidth of the generators.

$$\begin{cases} u_s = u_p > B_{\alpha,max}, & L = 243 \\ B_{\alpha,min} < u_s = u_p < B_{\alpha,max}, & L = 427, L = 711. \end{cases} \tag{62}$$

Fig. 11 and Fig. 12 show the recovery probability and the recovery NMSE for three types of generators. We think the proposed method can be put into practice when the recovery probability is greater than 0.9. The conditions of simulation are as follows: SNR is 20dB, the number of bands is 4, the number of channels varies from 4 to 60 with a step 2.

In Fig. 11, the recovery probability increases as the number of channels increasing for three curves. When the number of channels are 16, 20, 26 respectively, the recovery probability of three curves is the first time more than 0.9, as a result, the total sampling rates are 658.42MHz, 468.38MHz, 365.68MHz, the compressed ratio are 0.066, 0.047 and 0.036. Although the decrease of u_p and u_s results in the decrease of the total sampling rate, the system needs to increase number of channels to guarantee the successful recovery probability, also the increasing of the channels would increase the complexity of the design of the system.

Fig. 12 shows the recovery NMSE with three conditions of different numbers of generators, it is obvious the proposed method has higher precision when $u_s = u_p > B_{\alpha,max}$. According to simulation, the choice of the number of generators decides the performance of the proposed system, mostly, the number of generators is chosen to satisfy $u_s = u_p > B_{\alpha,max}$ to get better performance and easier implement with the expense of higher total sampling rate.

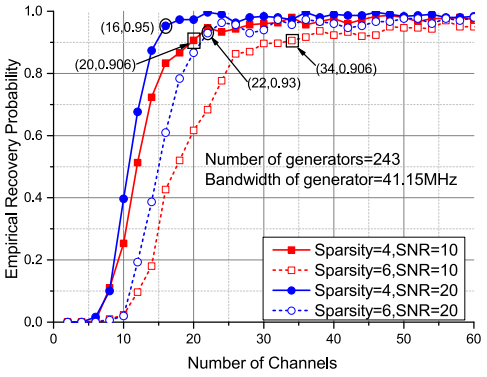

FIGURE 13. The recovery probability of the proposed method with different SNRs and sparsity.

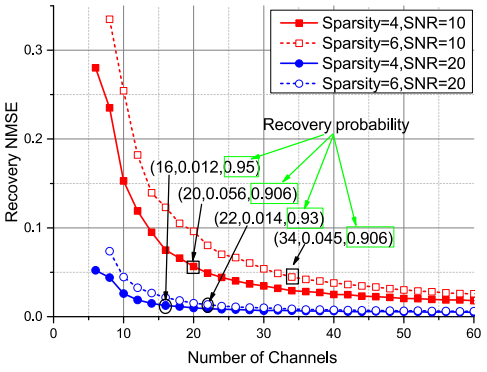

FIGURE 14. The recovery NMSE of the proposed method with different SNRs and sparsity.

The robustness and recovery accuracy are analyzed with different SNR, sparsity and number of channels. From previous simulation, the proposed method would get better performance when $u_s = u_p > B_{\alpha,max}$. We choose the number of the generators is 235. Fig. 13 and Fig. 14 show the recovery probability and recovery accuracy. The number of bands is {4, 6}. SNR is {10, 20}dB. The number of channels changes from 4 to 60 with a step 2. From Fig. 13 we can see the bigger SNR is, the better the proposed method is. The more sparsity needs more channels to get stable recovery. The curves are tend to be stable reconstruction when the numbers of channels reach to {16, 20, 22, 34}. From Fig. 14, the bigger SNR

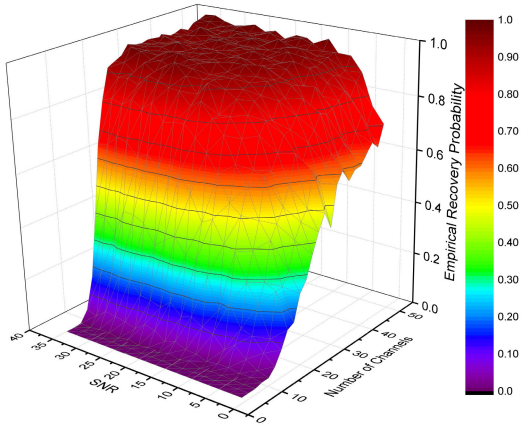

FIGURE 15. The robustness of the proposed system.

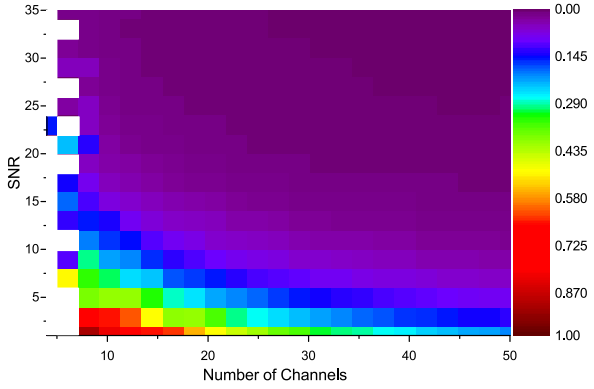

FIGURE 16. The accuracy of the proposed system.

is, the higher recovery accuracy is. The recovery accuracy tends to be stable as the increasing of the number of channels. From Fig. 13 and Fig. 14, the proposed system is useful for multiband signal in the FrFD.

Fig. 15 uses a 3D figure to depict the robustness of the proposed system, which is more detailed visual to see how the number of channels and SNR influence the performance of the proposed system. The colorbar stands for the recovery probability. The number of bands is 6. The number of channels varies from 4 to 50 with a step 2. The range of SNR is from 1 to 35 with a step 2. The probability of the successful recovery increases dramatically when the number of channels reaches the theoretical value which can be computed by ExRIP [26]. The recovery probability approached to 0.9 when the number of bands is 6 and the number of channels is 12, and experimental results is in good agreement with the theoretical value of number of channels. The number of channels is a decisive factor for the probability of the successful recovery.

The performance of recovery accuracy is shown in Fig. 16. The conditions are the same with Fig. 15. The colorbar stands for the NMSE. The range of the NMSE colorbar is from 0 to 1. The area of deep color represents a low NMSE and high recovery accuracy. The possible wrong indices in the recovered support and noise are the main error sources. The white region are zeros due to the recovery probability is zero.

V. CONCLUSION

This paper introduces a compressed sampling method of analog sparse signals, which combines the SI sampling space and compressed sensing in the FrFD. The SI sampling subspaces are extended from single generator model to a multiple generators model associated with the FrFT. The extended model derived a necessary and sufficient condition for transform fractional bandlimited signals to form an orthogonal basis or a Riesz basis for SI subspaces. Considering some specific sampled signals can be expressed by multiple generators, the sampled signals are sparse in the subspaces when taking the generators as sparse bases, as a result, some generators are not necessary. The compressed sampling methods make full use of the sparsity of the signals in the extended generalized subspaces. Considering the choices of generators are difficult, we average the whole sampled domain into many equal intervals, and all the intervals construct the sampling subspace. The simulations validate the correctness of theory in two aspects, first, the proposed sampling method based on the theorem of the generalized sampling spaces has higher recovery accuracy for multiband signals in the FrFD, second, the proposed compressed sampling method can sample and recover the multiband signals in the FrFD with a relatively low sampling rate.

REFERENCES

[1] L. B. Almeida, "The fractional Fourier transform and time-frequency representations," *IEEE Trans. Signal Process.*, vol. 42, no. 11, pp. 3084–3091, Nov. 1994.

[2] E. Sejdić, I. Djurović, and L. Stanković, "Fractional Fourier transform as a signal processing tool: An overview of recent developments," *Signal Process.*, vol. 91, no. 6, pp. 1351–1369, Jun. 2011.

[3] X. Li, H. Wang, and H. Luo, "Intra-pulse modulation recognition for fractional bandlimited signals based on a modified MWC-based digital receiver," *IEEE Access*, vol. 8, pp. 85067–85082, 2020.

[4] J. Xu, Y. Pi, and Z. Cao, "UWB LFM echo signal detection and time-delay estimation based on compressive sensing," in *Proc. IEEE 10th Int. Conf. SIGNAL Process.*, Oct. 2010, pp. 2435–2438.

[5] A. Bhandari and A. I. Zayed, "Shift-invariant and sampling spaces associated with the fractional Fourier transform domain," *IEEE Trans. Signal Process.*, vol. 60, no. 4, pp. 1627–1637, Apr. 2012.

[6] X. Liu, J. Shi, X. Sha, and N. Zhang, "A general framework for sampling and reconstruction in function spaces associated with fractional Fourier transform," *Signal Process.*, vol. 107, pp. 319–326, Feb. 2015.

[7] H. Zhao, L. Qiao, N. Fu, and G. Huang, "A generalized sampling model in shift-invariant spaces associated with fractional Fourier transform," *Signal Process.*, vol. 145, pp. 1–11, Apr. 2018.

[8] X.-G. Xia, "On bandlimited signals with fractional Fourier transform," *IEEE Signal Process. Lett.*, vol. 3, no. 3, pp. 72–74, Mar. 1996.

[9] R. Tao, B. Deng, W. Q. Zhang, and Y. Wang, "Sampling and sampling rate conversion of band limited signals in the fractional Fourier transform domain," *IEEE Trans. Signal Process.*, vol. 56, no. 1, pp. 158–171, Jan. 2008.

[10] A. Bhandari and P. Marziliano, "Sampling and reconstruction of sparse signals in fractional Fourier domain," *IEEE Signal Process. Lett.*, vol. 17, no. 3, pp. 221–224, Mar. 2010.

[11] J. Shi, G. Si, and Y. Zhang, "Application of fractional Fourier transform for prediction of ball mill loads using acoustic signals," *IEEE Access*, vol. 7, pp. 84170–84181, 2019.

[12] J. Shi, W. Xiang, X. Liu, and N. Zhang, "A sampling theorem for the fractional Fourier transform without band-limiting constraints," *Signal Process.*, vol. 98, pp. 158–165, May 2014.

[13] J. Shi, X. Liu, L. He, M. Han, Q. Li, and N. Zhang, "Sampling and reconstruction in arbitrary measurement and approximation spaces associated with linear canonical transform," *IEEE Trans. Signal Process.*, vol. 64, no. 24, pp. 6379–6391, Dec. 2016.
[14] A. Bhandari and A. I. Zayed, "Shift-invariant and sampling spaces associated with the special affine Fourier transform," *Appl. Comput. Harmon. Anal.*, vol. 47, no. 1, pp. 30–52, Jul. 2019.
[15] Y. C. Eldar and T. Michaeli, "Beyond bandlimited sampling," *IEEE Signal Process. Mag.*, vol. 26, no. 3, pp. 48–68, May 2009.
[16] A. G. Garcia, M. A. Hernandez-Medina, and G. Perez-Villalon, "Oversampling in shift-invariant spaces with a rational sampling period," *IEEE Trans. Signal Process.*, vol. 57, no. 9, pp. 3442–3449, Sep. 2009.
[17] T. Blumensath and M. E. Davies, "Sampling theorems for signals from the union of finite-dimensional linear subspaces," *IEEE Trans. Inf. Theory*, vol. 55, no. 4, pp. 1872–1882, Apr. 2009.
[18] Y. C. Eldar and M. Mishali, "Robust recovery of signals from a structured union of subspaces," *IEEE Trans. Inf. Theory*, vol. 55, no. 11, pp. 5302–5316, Nov. 2009.
[19] Y. C. Eldar, "Compressed sensing of analog signals in shift-invariant spaces," *IEEE Trans. Signal Process.*, vol. 57, no. 8, pp. 2986–2997, Aug. 2009.
[20] E. J. Candès, J. Romberg, and T. Tao, "Robust uncertainty principles: Exact signal reconstruction from highly incomplete frequency information," *IEEE Trans. Inf. Theory*, vol. 52, no. 2, pp. 489–509, Feb. 2006.
[21] D. L. Donoho, "Compressed sensing," *IEEE Trans. Inf. Theory*, vol. 52, no. 4, pp. 1289–1306, Jan. 2006.
[22] J. Shi, Y. Chi, and N. Zhang, "Multichannel sampling and reconstruction of bandlimited signals in fractional Fourier domain," *IEEE Signal Process. Lett.*, vol. 17, no. 11, pp. 909–912, Nov. 2010.
[23] D. Wei and Y.-M. Li, "Reconstruction of multidimensional bandlimited signals from multichannel samples in linear canonical transform domain," *IET Signal Process.*, vol. 8, no. 6, pp. 647–657, Aug. 2014.
[24] D. Wei and Y.-M. Li, "Generalized sampling expansions with multiple sampling rates for lowpass and bandpass signals in the fractional Fourier transform domain," *IEEE Trans. Signal Process.*, vol. 64, no. 18, pp. 4861–4874, Sep. 2016.
[25] M. Mishali and Y. C. Eldar, "Reduce and boost: Recovering arbitrary sets of jointly sparse vectors," *IEEE Trans. Signal Process.*, vol. 56, no. 10, pp. 4692–4702, Oct. 2008.
[26] M. Mishali and Y. C. Eldar, "Expected RIP: Conditioning of the modulated wideband converter," in *Proc. IEEE Inf. Theory Workshop (ITW)*, Taormina, Italy, Oct. 2009, pp. 343–347.

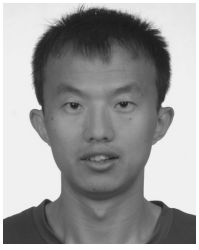

HAORAN ZHAO received the B.Sc., M.Sc., and Ph.D. degrees from the Harbin Institute of Technology, China, in 2010, 2012, and 2018, respectively. He is currently a Research Assistant at Tsinghua University. His research interests include high-speed digital design, massive storage, sparse signal processing, and automatic drive technology.

LEI ZHANG (Member, IEEE) received the B.S. and Ph.D. degrees (Hons.) from the Department of Electronic Engineering, Tsinghua University, Beijing, China, in 2003 and 2008, respectively. From 2006 to 2008, he was a Visiting Scholar under the joint degree program with the University of California at Los Angeles (UCLA), Los Angeles, CA, USA, where he was a Postdoctoral Fellow, from 2008 to 2010. Since 2010, he has been an Assistant Professor with the Institute of Microelectronics, Tsinghua University. Since 2012, he has also been an Associate Professor with the Institute of Microelectronics, Tsinghua University. He has authored or coauthored more than 100 technical articles and coauthored four technical books. He holds more than 20 patents. He has directed/participated in over 20 projects, including the National Basic Research Program of China, the National High-Tech Research and Development Program of China, NSFC, and the National Key Research and Development Program of China. His current research interests include analog and RF/mmW/THz integrated circuits and systems for sixth-generation (6G) wireless communications, terahertz imaging, fully integrated multichannel automotive radar, data converters, CMOS-integrated microarray biochips for bio-sensing and bio-detection, and machine learning algorithms. He is a member of the Analog Signal Processing Technical Committee (ASPTC) of the IEEE Circuits and Systems Society (CASS) and the National Intelligent Connected Vehicle Standardization Committee of China and a Technical Program Committee (TPC) Member of the IEEE Custom Integrated Circuit Conference (CICC). He was a recipient of six Provincial and Ministerial Science and Technology Awards of China and three International Conference Awards.

LIYAN QIAO (Member, IEEE) received the B.Sc., M.Sc., and Ph.D. degrees from the Harbin Institute of Technology (HIT), in 1996, 1998, and 2005, respectively. He is currently a Professor at HIT. His main research interests include signal processing, fractional Fourier transform, data acquisition technology, and mass storage data recording technology.